LETTER

doi:10.1038/nature15543

Observation of the competitive double-gamma nuclear decay

C. Walz[1], H. Scheit[1], N. Pietralla[1], T. Aumann[1], R. Lefol[1,2] & V. Yu. Ponomarev[1]

The double-gamma ($\gamma\gamma$)-decay of a quantum system in an excited state is a fundamental second-order process of quantum electrodynamics. In contrast to the well-known single-gamma (γ)-decay, the $\gamma\gamma$-decay is characterized by the simultaneous emission of two γ quanta, each with a continuous energy spectrum. In nuclear physics, this exotic decay mode has only been observed for transitions between states with spin-parity quantum numbers $J^\pi = 0^+$ (refs 1–3). Single-gamma decays—the main experimental obstacle to observing the $\gamma\gamma$-decay—are strictly forbidden for these $0^+ \rightarrow 0^+$ transitions. Here we report the observation of the $\gamma\gamma$-decay of an excited nuclear state ($J^\pi = 11/2^-$) that is directly competing with an allowed γ-decay (to ground state $J^\pi = 3/2^+$). The branching ratio of the competitive $\gamma\gamma$-decay of the $11/2^-$ isomer of ^{137}Ba to the ground state relative to its single γ-decay was determined to be $(2.05 \pm 0.37) \times 10^{-6}$. From the measured angular correlation and the shape of the energy spectra of the individual γ-rays, the contributing combinations of multipolarities of the γ radiation were determined. Transition matrix elements calculated using the quasiparticle–phonon model reproduce our measurements well. The $\gamma\gamma$-decay rate gives access to so far unexplored important nuclear structure information, such as the generalized (off-diagonal) nuclear electric polarizabilities and magnetic susceptibilities[3].

Two-photon processes, that is, excitation and decay of a quantum state simultaneously involving two photons whose energy sum $E_1 + E_2$ matches the transition energy E_0, have been studied intensely in the past two decades in atomic physics[4,5] and are now routinely applied in spectroscopic studies. These processes were first discussed theoretically in 1929[6,7], and the same approach predicted the existence of the rare double-β-decay of atomic nuclei as the analogous second-order process for the electroweak interaction[8]. In contrast to the situation in atomic physics, data on the $\gamma\gamma$-decay of atomic nuclei are very sparse. Up to now, $\gamma\gamma$-decays of nuclear states have only been observed for the special cases of the first excited states of the 'doubly-magic' nuclei ^{16}O, ^{40}Ca and ^{90}Zr (refs 1–3, 9). The first excited states of these nuclei have the unusual property of having spin-parity quantum numbers $J^\pi = 0^+$, which is also the case for their ground states. Hence, γ-decays are strictly forbidden for these transitions. For almost all other nuclei, the first excited states have spin quantum numbers larger than zero, making γ-decays possible. Despite several searches[10,11], the $\gamma\gamma$-decay has never been observed in a situation where a single γ-ray transition is allowed, a situation we call the competitive $\gamma\gamma$-decay, denoted by '$\gamma\gamma/\gamma$-decay'. Preliminary evidence for the $\gamma\gamma/\gamma$-process obtained by other groups in parallel with our work has been announced elsewhere (ref. 12, and D. J. Millener and R. J. Sutter (personal communication); ref. 13, and C. J. Lister (personal communication)). In the present work, the experimental difficulties have been overcome and we report here firm observation of the $\gamma\gamma/\gamma$-decay of a nuclear state.

The experimental challenge to the observation of the competitive $\gamma\gamma$-decay arises from its decay rate, which is more than five orders of magnitude smaller than that of the allowed γ-decay. In an ensemble of nuclei undergoing γ-decay from a given excited state, there are a large number of γ quanta being emitted, which cause two basic challenges, illustrated in Fig. 1. First, a γ quantum with transition energy E_0 can deposit part of its energy in one detector and then scatter into the second detector, depositing there its remaining energy. The sum of the energies registered in both detectors equals the transition energy, which is the signature of the $\gamma\gamma$-decay. Second, two γ quanta, each with energy E_0, can be emitted independently by two nuclei at almost the same time, and deposit a fraction of their energy in two detectors, such that the energy sum is again close to E_0. Although these random coincidences can be subtracted from truly simultaneous events, they cause a substantial statistical uncertainty, thereby preventing the observation of the much rarer $\gamma\gamma/\gamma$-decay unless they are suppressed properly.

In our experiment, the first excited $11/2^-$ state of ^{137}Ba was populated through β^- decays of ^{137}Cs nuclei, a well known γ-ray calibration standard. This isomer decays dominantly via a single-γ magnetic hexadecapole (M4) transition to the $3/2^+$ ground state, emitting a γ-ray with an energy of 661.66 keV (Fig. 2a inset). The emitted γ-rays were detected using five large-volume $LaBr_3$:Ce (Ce-activated $LaBr_3$) detectors positioned in a planar fashion symmetrically around the ^{137}Cs γ-ray source (Fig. 1a). Thus, the angle between two adjacent detectors amounted to 72°, and two groups of five detector pairs can be formed with relative angles of 72° ('72°-group') and 144° ('144°-group'). The undesired Compton scattering of 661.66-keV γ-rays between two detectors was suppressed by thick lead shields. Data were recorded for a measurement time of 52.7 days.

The spectrum of the time-difference (Δt) between two hits in two detectors of the 72°-group is presented in Fig. 1b inset. The prompt time-coincidence peak centred at $\Delta t = 0$ sits on a flat background caused by random coincidences. The time condition $|\Delta t| \leq 1.2$ ns selects true (prompt) as well as random coincidences, resulting in the energy-sum spectrum $E_1 + E_2$ shown in Fig. 1b (orange filled circles). The contribution of random coincidences is determined by imposing a wide time gate on the flat background and scaling the corresponding energy-sum spectrum with a factor of 0.0214 to correct for the different widths of both conditions (Fig. 1b, green filled triangles). The random coincidences dominate the statistical uncertainty.

The final energy-sum spectrum of the 72°-group—after subtraction of random coincidences—is shown in Fig. 2a. We imposed the energy condition $|E_1 - E_2| < 300$ keV to obtain further background suppression (see Supplementary Information). The spectrum is well described by assuming a superposition of an exponential background and a Gaussian peak at 661.6(1.6) keV in agreement with the expected energy sum (here and elsewhere, numerals in parentheses indicate the 1σ uncertainty). It has an area of 693(95) counts, establishing the observation of the competitive $\gamma\gamma$-decay.

Reasonable explanations other than $\gamma\gamma/\gamma$-decay can be excluded. First, let us assume that despite our careful assembly of the lead shields, the peak is caused by Compton-scattered 661.66-keV γ-rays (due, for example, to a small hole in the absorptive lead shields). The additional flight path of the γ quantum from one detector to the other would cause a time delay to which the $LaBr_3$:Ce detectors are sensitive. Hence,

[1]Institut für Kernphysik, Technische Universität Darmstadt, 64289 Darmstadt, Germany. [2]Department of Physics, University of Saskatchewan, Saskatoon S7N5E2, Canada.

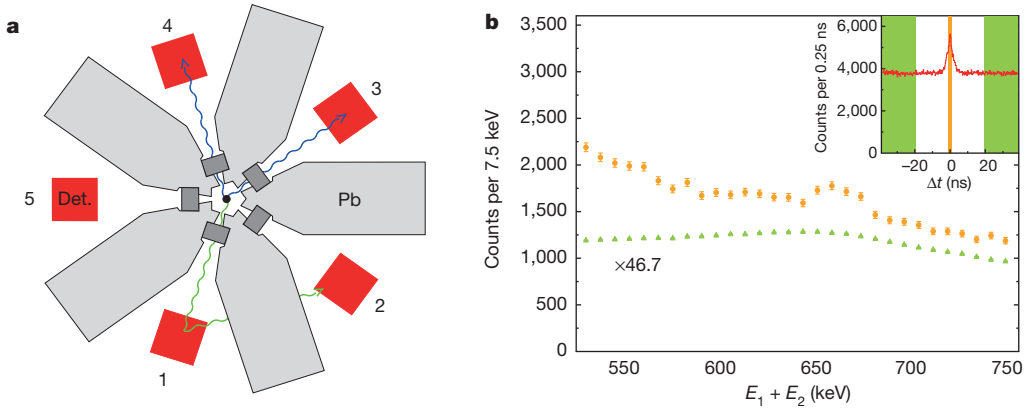

Figure 1 | The two main experimental obstacles to measuring the $\gamma\gamma/\gamma$-decay. a, Schematic illustration of the experimental set-up. A 661.66-keV γ-ray (green wavy line) emitted from the central source (black dot) can deposit part of its energy in detector 1 (labelled red square) and then be scattered into detector 2 where it deposits its remaining energy. Lead (grey) is used to suppress this effect relative to the $\gamma\gamma$-events (blue wavy lines). Lead collimators (dark grey) are used for background suppression. **b**, Energy-sum spectra of the 72°-group with time gates on the prompt coincidence peak (orange filled circles; $|\Delta t| \leq 1.2$ ns) and on the random coincidences (green filled triangles; 20 ns $\leq |\Delta t| \leq$ 76 ns). The ordinate values should be multiplied by the given factor. Inset, time difference spectrum (red trace) and parts of the imposed time gates (orange bar (prompt) and green areas (random)) used to obtain the energy-sum spectra of **b**. The energy condition $|E_1 - E_2| < 300$ keV was imposed on data reported in **b** as well as on that shown in the inset. Error bars, ±1 s.d.

this possibility can be excluded by investigating the shape of the time-difference spectra. A narrow energy gate on the $\gamma\gamma/\gamma$-sum-energy peak results in the time-difference spectrum presented in Fig. 2b (orange filled circles). The contribution of the background counts (solid green curve) is determined with energy gates on the background. The time-difference spectrum follows a Gaussian distribution centred at $\Delta t = 0$ (solid orange curve) with a full-width at half-maximum that is in agreement with the time resolution of our $LaBr_3$:Ce detectors, namely 1 ns. In the case of Compton scattering, a superposition of two Gaussians with centroids at $\Delta t = \pm 0.8$ ns (solid red curve in Fig. 2b) would be expected, in contradiction to the observed time spectrum.

A second possibility for the origin of the peak is a sequential decay via the $1/2^+$ state at an excitation energy of 283.5 keV (Fig. 2a inset), corresponding to two subsequent γ-decays. Our observed γ-ray energy spectra of individual photons—gated on $\gamma\gamma/\gamma$-events—are continuous and do not peak at the transition energies to and from the $1/2^+$ state, thereby excluding sequential decay. In addition, the γ-branch to the $1/2^+$ state has been measured recently and amounts to only $1.12(9) \times 10^{-7}$ (ref. 14), less than 6% of our measured $\gamma\gamma/\gamma$-branching ratio.

In addition, data were recorded for the detector group forming opening angles of 144°. A Gaussian peak is found in the corresponding energy-sum spectrum at an energy of 664.2(28) keV and with an area of 307(78) counts (Fig. 3). This shows that the $\gamma\gamma/\gamma$-decay of the $11/2^-$ isomer of ^{137}Ba exhibits a very pronounced angular correlation of the two emitted γ quanta, characteristic of the multipolarities involved in the transition.

In the theoretical treatment of the $\gamma\gamma$-decay process, it follows from second-order perturbation theory that the calculation of the $\gamma\gamma$-decay transition rate[3,15] involves a summation over a complete set of states, subject to well known electromagnetic selection rules based on the multipolarity and character of the transition. In a reasonable approximation, the possible decay paths can be restricted to two cases (see Supplementary Information for a justification of this approximation), which we will describe here in the language of

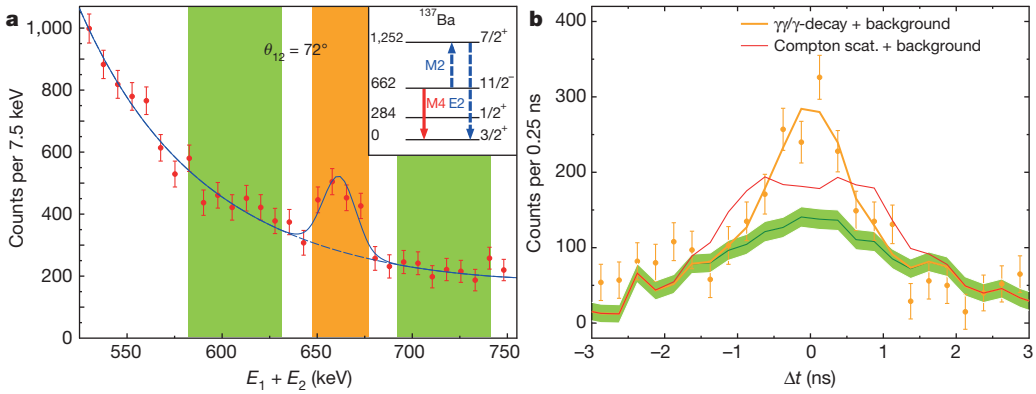

Figure 2 | Energy-sum spectrum and energy-gated time spectra of the 72°-group. a, Energy-sum spectrum $E_1 + E_2$ after subtraction of the random coincidences (requiring the energy condition $|E_1 - E_2| < 300$ keV). The spectrum is fitted with a superposition of a Gaussian and an exponential function to describe the peak and the background, respectively. The orange (647 keV $< E_1 + E_2 <$ 677 keV) and green areas (582 keV $< E_1 + E_2 <$ 632 keV and 692 keV $< E_1 + E_2 <$ 742 keV) represent the energy conditions employed to obtain the time-difference spectra displayed in **b**. Inset, level scheme of ^{137}Ba with level energies in keV on the left and spin-parity J^π quantum numbers on the right. The solid red arrow labels the single-γ transition of the $11/2^-$ state to the ground state. The dashed blue arrows illustrate the structure of the matrix element of the $\gamma\gamma/\gamma$-decay involving the lowest $7/2^+$ state. **b**, Time difference spectra. The orange data points correspond to the orange region in **a**, while the green solid line with surrounding shading shows the background corresponding to the green area in **a**. The solid orange curve shows the expected time spectrum for $\gamma\gamma$-decay, while the solid red curve shows the expected time spectrum, assuming the peak at 661.66 keV was caused by Compton-scattered γ-rays. Error bars in **a**, **b** are ±1 s.d.

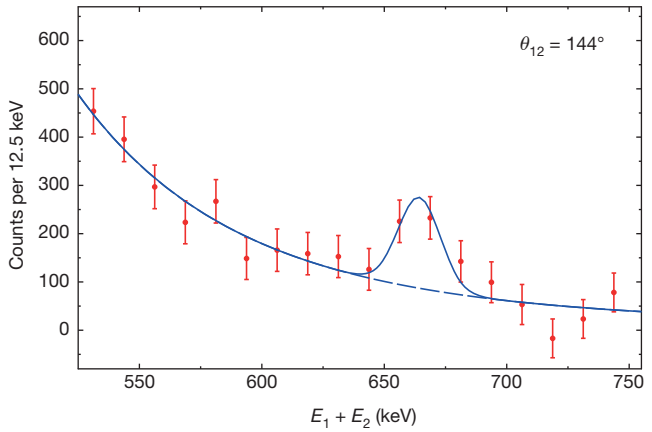

Figure 3 | Energy-sum spectrum of the 144°-group. The energy-sum spectrum $E_1 + E_2$ of the 144°-group after subtraction of the random coincidences (with the energy condition $|E_1 - E_2| < 250$ keV) is shown by the red data points. The Gaussian (solid blue curve) on top of an exponential background (dashed-blue curve) with a peak area of 307(78) counts is located at an energy of 664.2(28) keV, in agreement with the transition energy of 661.66 keV. Error bars, ±1 s.d.

'Feynman diagrams': in the first case, the nucleus undergoes virtual M2 transitions from the $11/2^-$ state to intermediate $7/2^+$ states (Fig. 2a inset), which are coupled by E2 transitions to the $3/2^+$ ground state. The final matrix element is obtained by a summation over all intermediate $7/2^+$ states of ^{137}Ba, whose contributions add up coherently. The second possibility is an E3M1 transition through intermediate $5/2^+$ states. The theory of the $\gamma\gamma$-decay is fully developed (see, for example, the Appendix of ref. 3; a first application of the formalism to ^{137}Ba was performed by D.J. Millener (personal communication)), and the differential branching ratio for the current case is approximately given by

$$\frac{\mathrm{d}^5\Gamma_{\gamma\gamma}}{\mathrm{d}\omega\mathrm{d}\Omega\mathrm{d}\Omega'} = A_{\mathrm{qq}}(\alpha^2_{\mathrm{E2M2}}, s) + A_{\mathrm{od}}(\alpha^2_{\mathrm{M1E3}}, s) + A_x(\alpha_{\mathrm{E2M2}}\alpha_{\mathrm{M1E3}}, s) \quad (1)$$

where $\Gamma_{\gamma\gamma}$ is the decay width for two-photon emission, and s stands for $\{L, L', I_n, \omega, \theta_{12}\}$; here L and L' label the multipoles of the two virtual transitions involved, I_n is the spin of the intermediate state n, ω is the energy of one of the γ-rays, θ_{12} denotes the angle between the two emitted γ-rays (that is, in our experiment $\theta_{12} = 72°$ and 144°) and $\mathrm{d}\Omega$ and $\mathrm{d}\Omega'$ are their solid angle elements. The coefficients α_{E2M2} and α_{M1E3} contain the nuclear structure information and are defined as

$$\alpha_{S'L'SL} = \sum_n \frac{\left\langle \frac{3}{2}^+ \| S'L' \| I_n \right\rangle \cdot \left\langle I_n \| SL \| \frac{11}{2}^- \right\rangle}{E_n - 0.5E_0} \quad (2)$$

where S and S' are the multipole characters. Each intermediate state $|I_n\rangle$ contributes with a product of matrix elements connecting it to the ground state ($\langle 3/2^+ \| S'L' \| I_n \rangle$) and to the $11/2^-$ isomer ($\langle I_n \| SL \| 11/2^- \rangle$) weighted approximately with the inverse of its excitation energy E_n. The quadrupole–quadrupole (A_{qq}) and octupole–dipole (A_{od}) terms of equation (1) depend only on α^2_{E2M2} and α^2_{M1E3}, respectively, while the interference term A_x depends on their product. Each term has a characteristic dependence on θ_{12} and the γ-ray energy ω. Thus, the values of α_{E2M2}, α_{M1E3} and the sign of $\alpha_{\mathrm{E2M2}}\alpha_{\mathrm{M1E3}}$ can be determined from an analysis of the measured angular correlation and the energy spectra of the emitted γ-rays. More information and the full form of equation (1) is given in Supplementary Information.

In Fig. 4, the result of a simultaneous fit to the energy spectrum (Fig. 4a) and angular correlation (Fig. 4b) is presented. The available data are well described by equation (1) (solid blue curve), and the contribution of the A_{qq} term (dashed blue curve) dominates in comparison to the A_{od} term (dotted blue curve). The angular correlation is very sensitive to the product of α_{E2M2} and α_{M1E3}. The final branching ratio amounts to $\Gamma_{\gamma\gamma}/\Gamma_\gamma = 2.05(37) \times 10^{-6}$, and the values for the two matrix elements are given in Table 1.

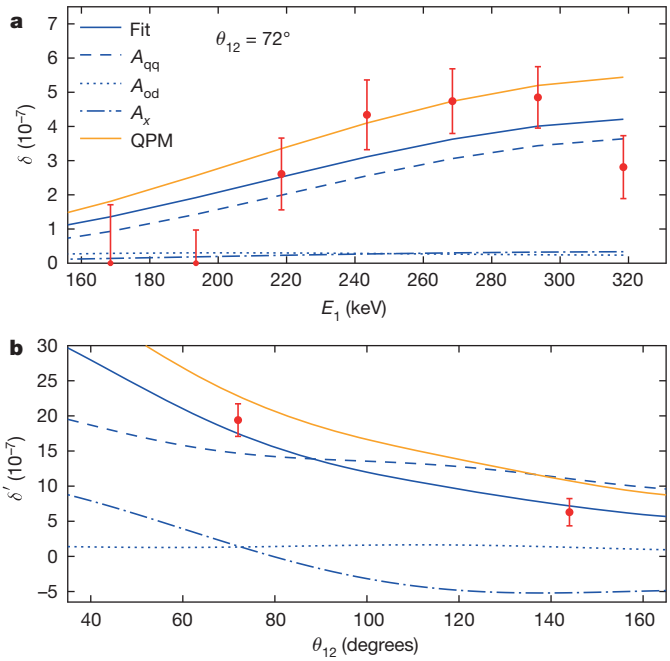

Figure 4 | Measured energy spectrum and angular correlation. δ (δ') is the differential $\gamma\gamma$-decay width from equation (1) integrated over the corresponding energy bin, divided by the γ-decay width Γ_γ and evaluated at the average emission angles $\theta_{12} = 72°$ and 144° (see Supplementary Information equation (2) for details of δ and δ'). **a**, Data points, dependence of δ on the energy E_1 of the lower-energy γ-ray for $\theta_{12} = 72°$. Also shown are the results of the fit of equation (1) (solid blue curve) and the contributions of the A_{qq} (dashed blue curve), A_{od} (blue dotted curve) and A_x terms (blue dash-dotted curve). Results of the QPM calculation (orange solid curve) are compared to the data. **b**, Data points, dependence of δ' on θ_{12} integrated over the energy bin $|E_1 - E_2| < 250$ keV. Other curves as in **a**. All values are corrected for the small contribution of the cascade of the decay via the $1/2^+$ state. Error bars, ±1 s.d.

In Fig. 4 and Table 1 our data are also compared to predictions of the microscopic quasiparticle–phonon model (QPM)[16] (solid orange curves). Further details of the QPM calculation are given in Supplementary Information. The QPM reproduces the experimental branching ratio and the two matrix elements rather well. As experimentally observed, it predicts a dominant A_{qq} term and a positive sign for $\alpha_{\mathrm{E2M2}}\alpha_{\mathrm{M1E3}}$. According to the QPM results, the value of α_{E2M2} is dominated by the matrix element coupled to the lowest $7/2^+$ state at an excitation energy of 1,252 keV (Supplementary Information). The reason is twofold: the lowest $7/2^+$ is close in energy to the $11/2^-$ state, reducing the size of the denominator in equation (2), and almost all of the low-lying E2-strength is concentrated in the $3/2^+ \rightarrow 7/2^+_1$ transition, resulting in a large $\langle 3/2^+ \| \mathrm{E2} \| 7/2^+_1 \rangle$ matrix element.

In conclusion, we have observed the $\gamma\gamma$-decay of a nuclear transition in competition with an allowed γ-decay. Our results demonstrate that theory provides a realistic description of the double-photon decay, and that the present state of the art of experimental equipment allows such a process to be measured even in the presence of the direct one-photon

Table 1 | Measured and theoretical parameter values

Parameter	Experiment	QPM theory
$\Gamma_{\gamma\gamma}/\Gamma_\gamma$ (10^{-6})	2.05(37)	2.69
α_{E2M2}(e^2 fm^4 MeV^{-1})	+33.9(2.8)	+42.60
α_{M1E3}(e^2 fm^4 MeV^{-1})	+10.1(4.2)	+9.50

See text for details of parameters. The uncertainties include the statistical error from the fit (±1 s.d.) and systematic contributions.

decay. This opens a new field of studies that were not previously possible. While the branching ratio is probably too small for the observation of the $\gamma\gamma$-decay of a first excited 2^+ state, which is present in nearly all even–even nuclei, we expect that there are other odd-A nuclei where the competitive $\gamma\gamma$-decay can be measured. Such experiments will be difficult and time-consuming, and the number of suitable nuclides obtainable in an isomeric state is limited. Nevertheless, the sensitivity of the experiment is now sufficient to enable investigation of so-far-unexplored nuclear structure observables, namely the (off-diagonal) nuclear electric and magnetic polarizabilities.

Received 13 May; accepted 27 August 2015.

1. Watson, B. A., Bardin, T. T., Becker, J. A. & Fisher, T. R. Two-photon decay of the 6.05-MeV state of ^{16}O. *Phys. Rev. Lett.* **35,** 1333–1336 (1975).
2. Schirmer, J. *et al.* Double gamma decay in ^{40}Ca and ^{90}Zr. *Phys. Rev. Lett.* **53,** 1897–1900 (1984).
3. Kramp, J. *et al.* Nuclear two-photon decay in $0^+ \rightarrow 0^+$ transitions. *Nucl. Phys. A* **474,** 412–450 (1987).
4. Mokler, P. H. & Dunford, R. W. Two-photon decay in heavy atoms and ions. *Phys. Scr.* **69,** C1–C9 (2004).
5. Ilakovac, K., Uroic, M., Majer, M., Pasic, S. & Vukovic, B. Two-photon decay of k-shell vacancy states in heavy atoms. *Radiat. Phys. Chem.* **75,** 1451–1460 (2006).
6. Göppert, M. Über die Wahrscheinlichkeit des Zusammenwirkens zweier Lichtquanten in einem Elementarakt. *Naturwissenschaften* **17,** 932 (1929).
7. Göppert-Mayer, M. Über Elementarakte mit zwei Quantensprüngen. *Ann. Phys.* **401,** 273–294 (1931).
8. Göppert-Mayer, M. Double beta-disintegration. *Phys. Rev.* **48,** 512–516 (1935).
9. Hayes, A. C. *et al.* Two-photon decay of the first excited 0^+ state in ^{16}O. *Phys. Rev. C* **41,** 1727–1735 (1990).
10. Beusch, W. Über Zweiquanten-Übergänge an Ba^{137}. *Helv. Phys. Acta* **33,** 363–394 (1960).
11. Basenko, V. K., Berlizov, A. N. & Prokopets, G. A. Estimation of the probability of two-photon decay of the 0.662 MeV ^{137}Ba state. *Bull. Russ. Acad. Sci. Phys.* **56,** 94 (1992).
12. Millener, D. J., Sutter, R. J. & Alburger, D. E. 2-gamma decay of the 662-keV isomer in ^{137}Ba. *Bull. Am. Phys. Soc.* **56,** DNP.CF.8 (2011); available at http://meetings.aps.org/link/BAPS.2011.DNP.CF.8 (2011).
13. Lister, C. J. *et al.* A search for 2-photon emission from the 662 keV state in ^{137}Ba. *Bull. Am. Phys. Soc.* **58,** DNP.CE.3 (2013); available at http://meetings.aps.org/link/BAPS.2013.DNP.CE.3 (2013).
14. Moran, K. *et al.* $E5$ decay from the $J^\pi = 11/2^-$ isomer in ^{137}Ba. *Phys. Rev. C* **90,** 041303 (2014).
15. Friar, J. L. Low-energy theorems for nuclear Compton and Raman scattering and $0^+ \rightarrow 0^+$ two-photon decays in nuclei. *Ann. Phys.* **95,** 170–201 (1975).
16. Soloviev, V. G. *Theory of Atomic Nuclei: Quasiparticles and Phonons* (Institute of Physics Publishing, Bristol, 1992).

Supplementary Information is available in the online version of the paper.

Acknowledgements This work was supported by the State of Hesse under the Helmholtz International Center for FAIR (HIC for FAIR) and by the German Research Council (DFG) under grant no. SFB 634. We thank D. J. Millener, R. J. Sutter for an open discussion and for generously sharing their preliminary results before publication, and C. J. Lister for discussions. H.S. thanks Dirk Schwalm for raising interest in this topic.

Author Contributions C.W. and H.S. performed the data analysis and derived the equations given in Supplementary Information. C.W., H.S. and N.P. contributed to the interpretation of the results. C.W. and R.L. were responsible for the set-up of the $LaBr_3$:Ce detector array and the data acquisition system. V.Yu.P. performed the QPM calculation. C.W., H.S., N.P. and T.A. prepared the manuscript. All authors discussed the results, commented on and contributed to the manuscript.

Author Information Reprints and permissions information is available at www.nature.com/reprints. The authors declare no competing financial interests. Readers are welcome to comment on the online version of the paper. Correspondence and requests for materials should be addressed to H.S. (hscheit@ikp.tu-darmstadt.de).